Dept. of Cranio-Maxillofacial and Oral Surgery

Oral Biotechnology & Bioengineering

3D-printed bone substitutes From pores to adaptive density minimal surface microarchitectures

Franz E. Weber
Prof. Dr. rer. nat. habil.

Universität Zürich
USZ Universitäts Spital Zürich

Hierarchy of bone structure

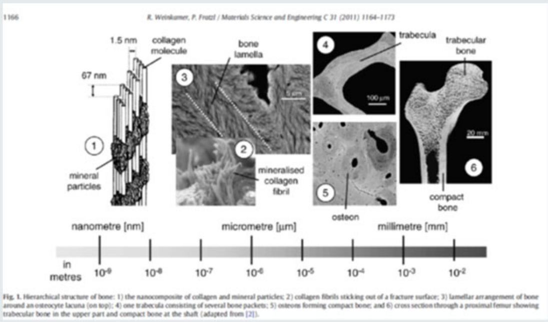

Bone remodeling

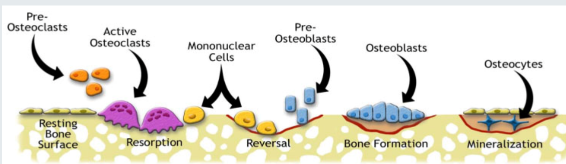

University of Michigan. http://www.umich.edu/news/index.html?Releases/2005/Feb05/r022005

Osteoclast

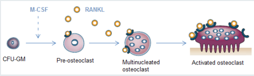

University of Michigan. http://www.umich.edu/news/index.html?Release

RB: ruffeled border
BL: basolateral membrane
FSD: functional secretory domain
VT: vesicular transport (transcytosis)

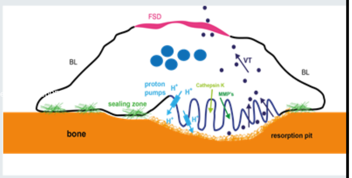

Modified from W.J. Boyle, 2003; H.K. Väänänen, 2000.

Osteoclast in action

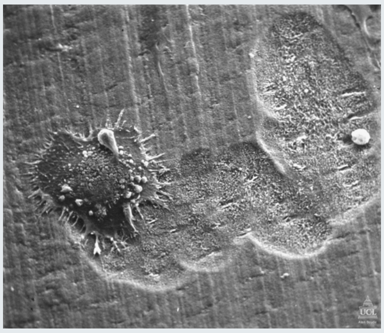

Breakfast, lunch and dinner for an osteoclast!
Alan Boyde, Bone Research Society

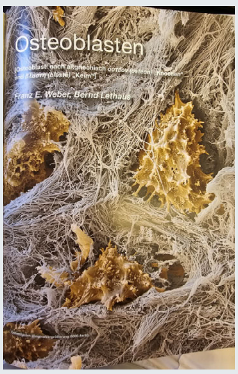

Mineralizing osteoblast

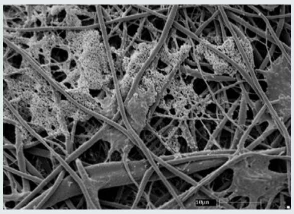

Weber FE and Lethaus B (2022) Osteoblast. Cell-to-Cell Communication: Cell-Atlas - Visual Biology in Oral Medicine ed. Gruber, Stadlinger, Terhyden
QUINTESSENCE PUBLISHING DEUTSCHLAND ISBN: 978-1-78698-107-3 or
QUINTESSENCE PUBLISHING Great Britain ISBN: 978-1-78698-107-3.

Bone remodeling depends on mechanical load

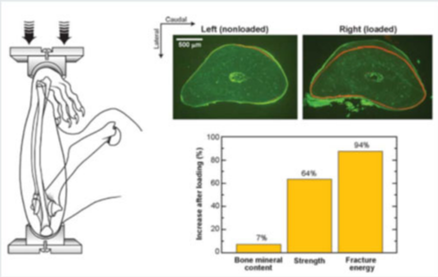

Biomechanical and Molecular Regulation of Bone Remodeling

Osteocyte senses load

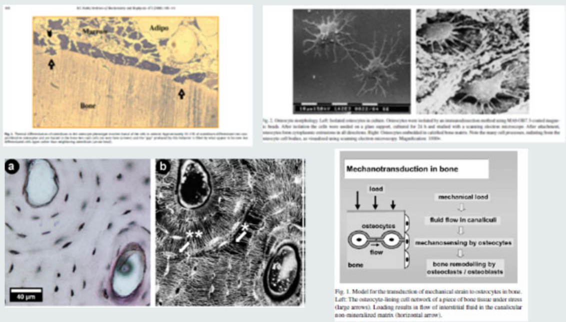

Osteocyte orchestrates bone remodeling

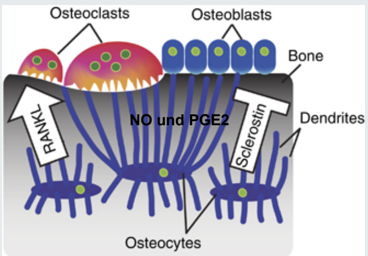

Nakashima T, et al. Nat Med 2011;17:1231–1234.

Autologous bone is still the gold standard bone substitute

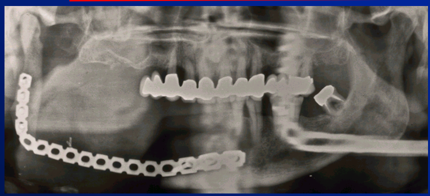

Mandibular reconstruction following tumor resection by using titanium plates and screws

Osteoconduction

TISSUE ENGINEERING: Part B
Volume 25, Number 5, 2019

DOI: 10.1089/ten.teb.2019.0047

termis. Tissue Engineering & Regenerative Medicine International Society

REVIEW ARTICLE

Reconsidering Osteoconduction in the Era of Additive Manufacturing

Franz E. Weber, PhD[1,2,3]

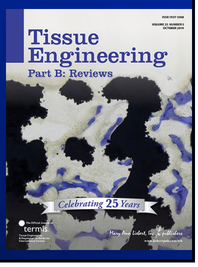

Osteoconduction:

Three-dimensional process of ingrowth of sprouting capillaries, perivascular tissue, and osteoprogenitor cells from a **bony bed** into the three-dimensional structure of a porous implant to use it as **guiding cue** to **bridge the defect** with bony tissue.

Osteoconduction myths

bone to implant contact (BIC)

Titan

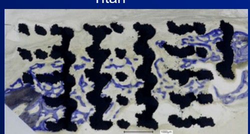

The initial formed woven bone (blue) lays mainly between the titanium surfaces and is covered with later formed lamellar bone (greyish-light blue)

CaP

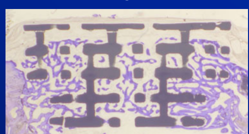

In areas with bone and material, bone to implant contact is only 10-20% of the implant surface

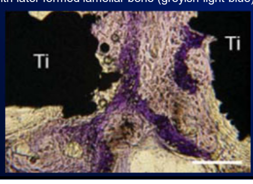

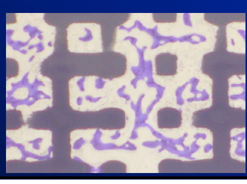

Osteoconduction

TISSUE ENGINEERING: Part B
Volume 25, Number 5, 2019
© Mary Ann Liebert, Inc.
DOI: 10.1089/ten.teb.2019.0047

termis
Tissue Engineering & Regenerative Medicine International Society

REVIEW ARTICLE

Reconsidering Osteoconduction in the Era of Additive Manufacturing

Franz E. Weber, PhD[1,2,3]

Osteoconduction:

Three-dimensional process of ingrowth of sprouting capillaries, perivascular tissue, and osteoprogenitor cells from a **bony bed** into the three-dimensional structure of a porous implant to use it as **guiding cue** to **bridge the defect** with bony tissue.

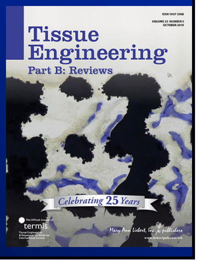

Autologous bone is still the gold standard bone substitute

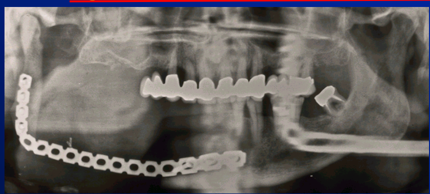

Mandibular reconstruction following tumor resection by using titanium plates and screws

Fibula (Wadenbein)

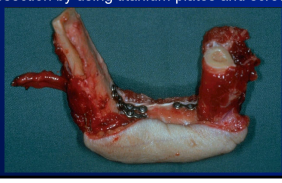

Principles of bone tissue engineering

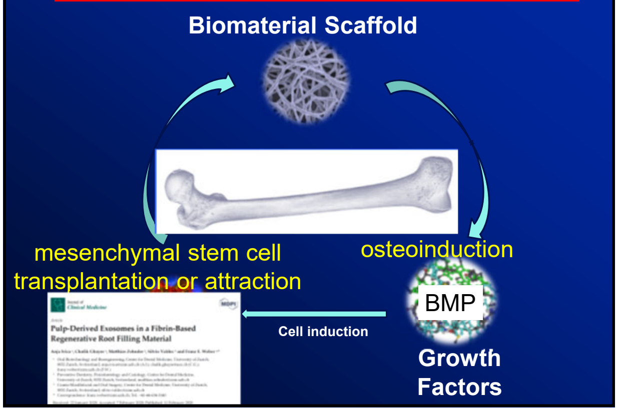

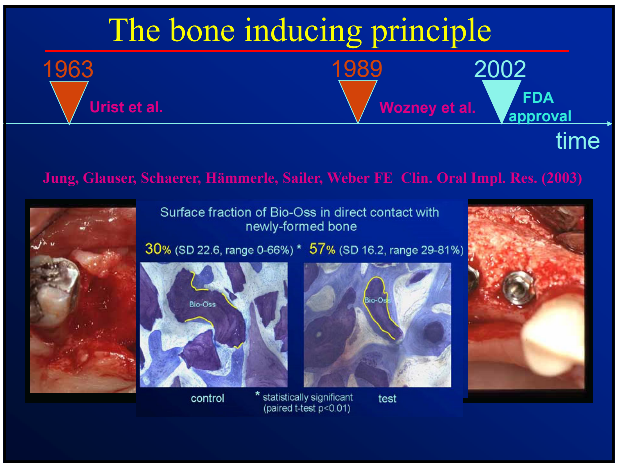
The bone inducing principle
1963
Urist et al.
1989
Wozney et al.
2002
FDA
approval
time
Jung, Glauser, Schaerer, Hämmerle, Sailer, Weber FE Clin. Oral Impl. Res. (2003)
Surface fraction of Bio-Oss in direct contact with
newly-formed bone
30% (SD 22.6, range 0-66%) * 57% (SD 16.2, range 29-81%)
control
* statistically significant
(paired t-test p<0.01)
test

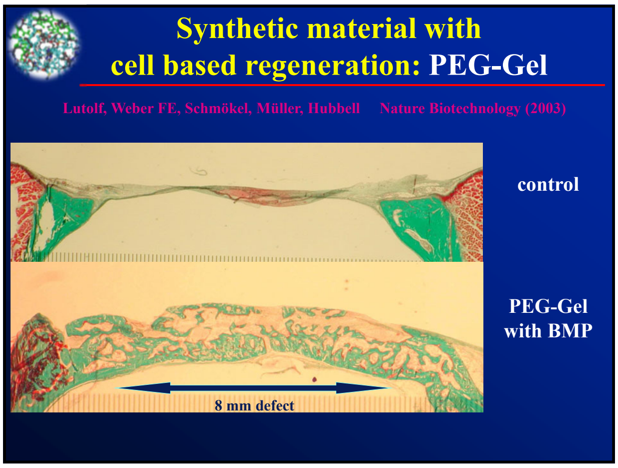
Synthetic material with
cell based regeneration: PEG-Gel
Lutolf, Weber FE, Schmökel, Müller, Hubbell Nature Biotechnology (2003)
control
PEG-Gel
with BMP
8 mm defect

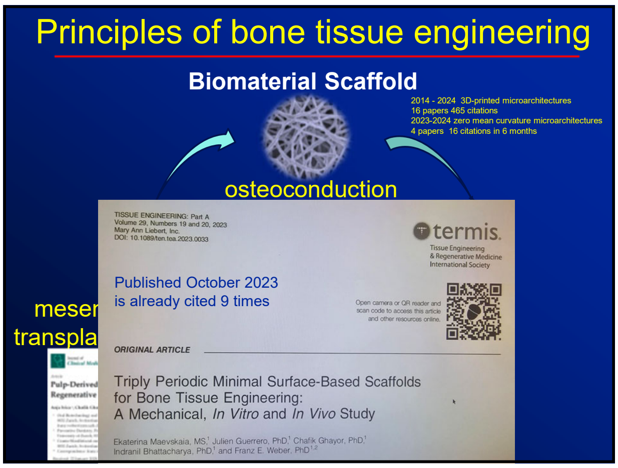
Principles of bone tissue engineering
Biomaterial Scaffold
2014 - 2024 3D-printed microarchitectures
16 papers 465 citations
2023-2024 zero mean curvature microarchitectures
4 papers 16 citations in 6 months
osteoconduction
TISSUE ENGINEERING: Part A
Volume 29, Numbers 19 and 20, 2023
Mary Ann Liebert, Inc.
termis
Published October 2023
is already cited 9 times
ORIGINAL ARTICLE
Triply Periodic Minimal Surface-Based Scaffolds
for Bone Tissue Engineering:
A Mechanical, In Vitro and In Vivo Study
Ekaterina Maevskaia, MS, Julien Guerrero, PhD, Chafik Ghayor, PhD,
Indranil Bhattacharya, PhD, and Franz E. Weber, PhD

Additive manufacturing

Source: Rapid manufacturing association

Additive Manufacturing of bone substitutes

Micro architecture

Conventional porous bone substitutes

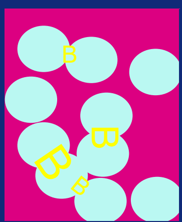

bone substitutes by additive manufacturing

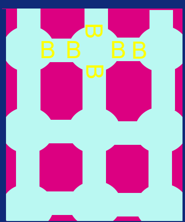

- Pores randomly distributed
- Bottle necks vary in size

- defined location of pores
- defined bottle necks

Additive manufacturing Integration into clinical workflow

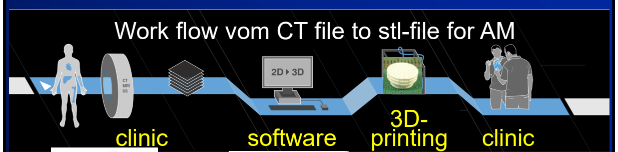

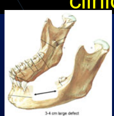

materialise
innovators you can count on

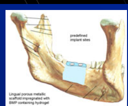

Information about the defect dimension = macroarchitecture of the defect

Stl-file with information of the macroarchitecture of the defect enables the production of personalized bone substitutes

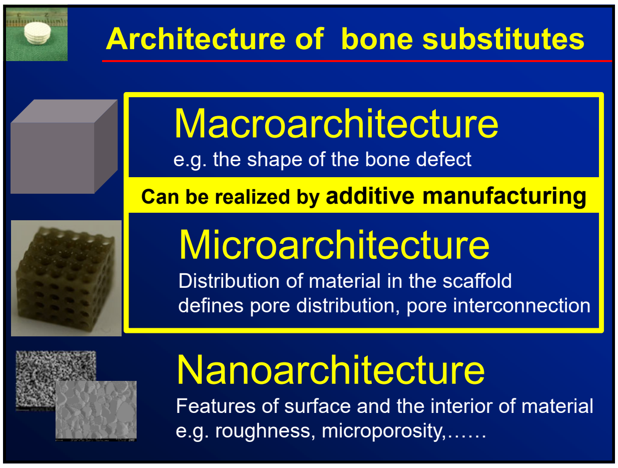
Architecture of bone substitutes
Macroarchitecture
e.g. the shape of the bone defect
Can be realized by additive manufacturing
Microarchitecture
Distribution of material in the scaffold
defines pore distribution, pore interconnection
Nanoarchitecture
Features of surface and the interior of material
e.g. roughness, microporosity,……

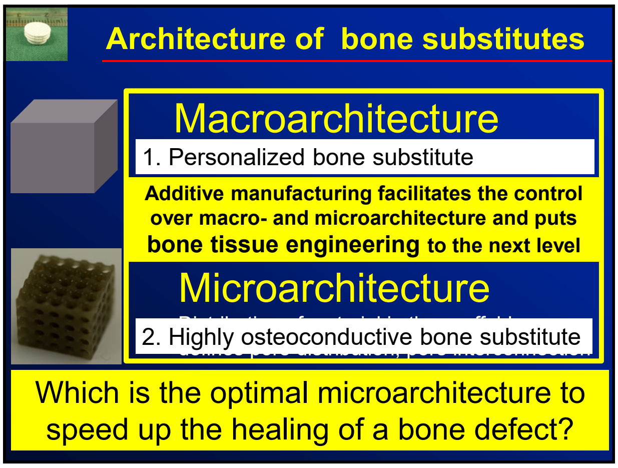
Architecture of bone substitutes
Macroarchitecture
1. Personalized bone substitute
Additive manufacturing facilitates the control over macro- and microarchitecture and puts bone tissue engineering to the next level
Microarchitecture
2. Highly osteoconductive bone substitute
Which is the optimal microarchitecture to speed up the healing of a bone defect?

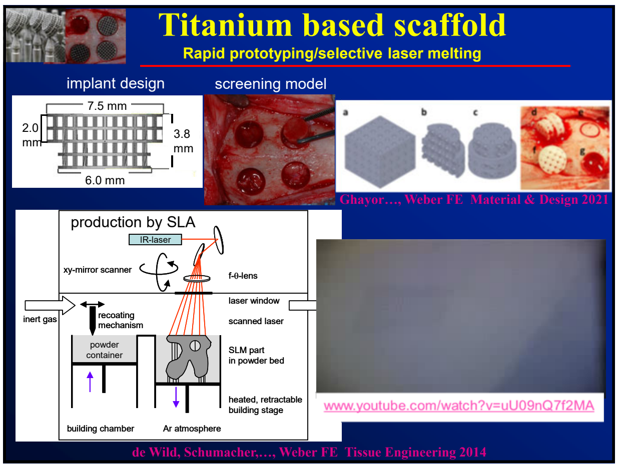
Titanium based scaffold
Rapid prototyping/selective laser melting
implant design
screening model
7.5 mm
2.0 mm
3.8 mm
6.0 mm
a
b
c
d
e
f
g
Ghayor…, Weber FE Material & Design 2021
production by SLA
IR-laser
xy-mirror scanner
f-θ-lens
laser window
scanned laser
inert gas
recoating mechanism
powder container
SLM part in powder bed
heated, retractable building stage
building chamber
Ar atmosphere
www.youtube.com/watch?v=uU09nQ7f2MA
de Wild, Schumacher,…, Weber FE Tissue Engineering 2014

Titanium based scaffold: lattice

Rapid prototyping/selective laser melting

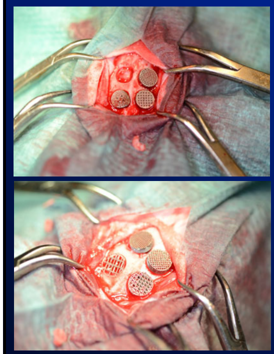

de Wild, ..Weber 3DPrinting&AM (2018)

Titanium based scaffold: lattice

Rapid prototyping/selective laser melting

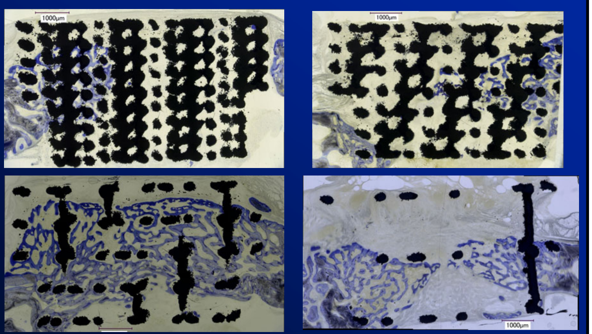

de Wild, ..Weber 3DPrinting & Additive manufacturing (2018)

Titanium based scaffold: lattice

Rapid prototyping/selective laser melting

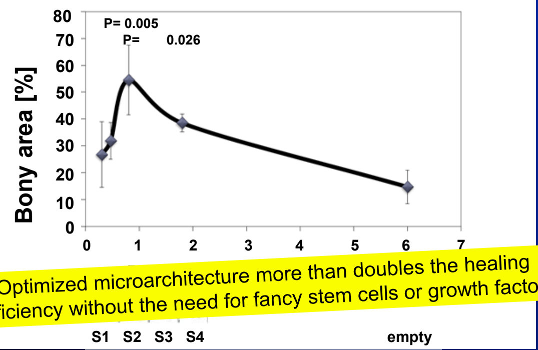

Optimized microarchitecture more than doubles the healing efficiency without the need for fancy stem cells or growth factors

de Wild, ..Weber 3DPrinting & Additive manufacturing (2018)

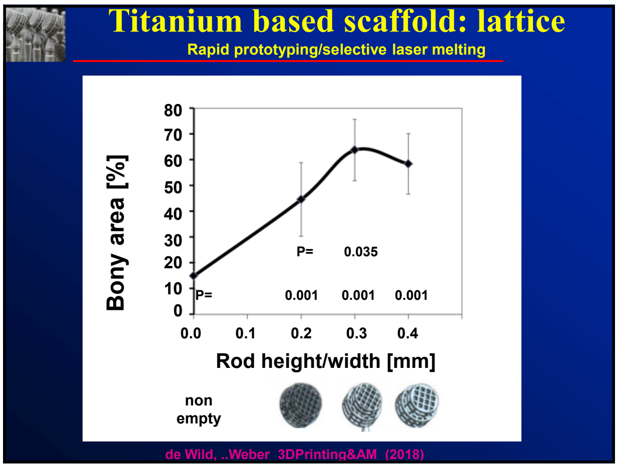
Titanium based scaffold: lattice
Rapid prototyping/selective laser melting
Bony area [%]
80
70
60
50
40
30
20
10
0
P=
P=
0.035
0.001
0.001
0.001
0.0
0.1
0.2
0.3
0.4
Rod height/width [mm]
non
empty
de Wild, ..Weber 3DPrinting&AM (2018)

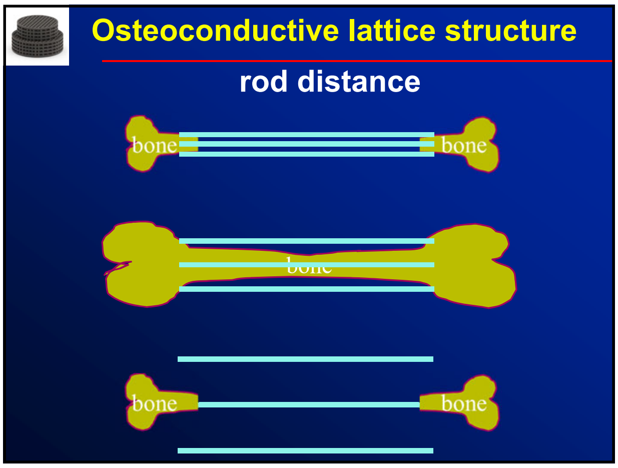
Osteoconductive lattice structure
rod distance
bone
bone
bone
bone
bone

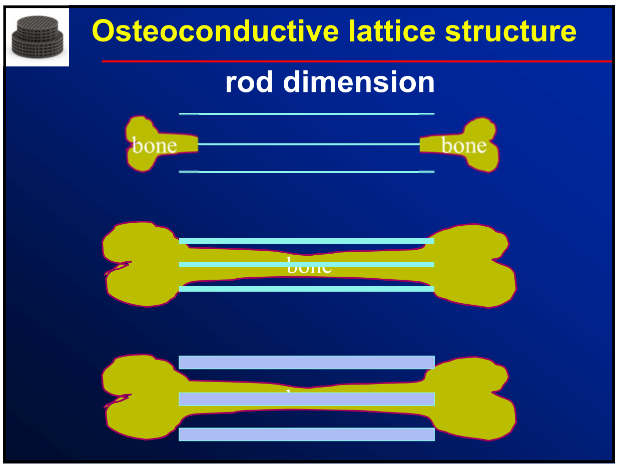
Osteoconductive lattice structure
rod dimension
bone
bone

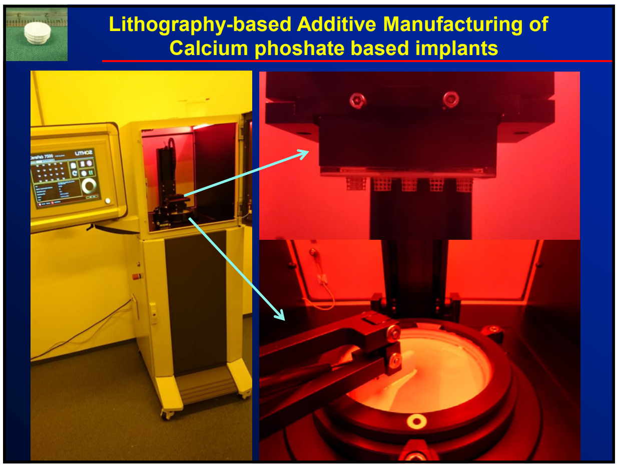
Lithography-based Additive Manufacturing of
Calcium phoshate based implants


Lithography-based Additive Manufacturing of
Calcium phoshate based implants

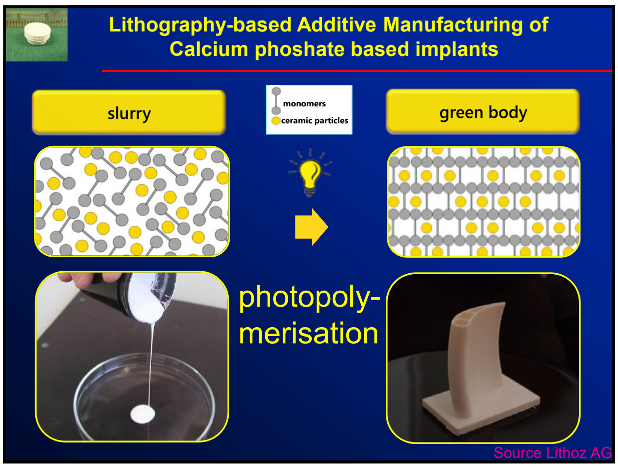
Lithography-based Additive Manufacturing of
Calcium phoshate based implants
slurry
monomers
ceramic particles
green body
photopoly-
merisation
Source Lithoz AG

Lithography-based Additive Manufacturing of Calcium phoshate based implants

Post processing of the green body

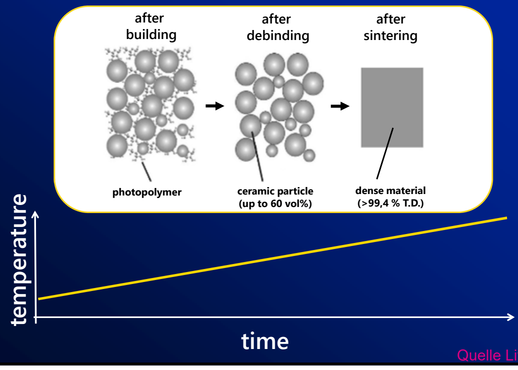

Quelle Lithoz AG

Lithography-based Additive Manufacturing of Calcium phoshate based implants

Debinding and sintern yields in:

1. Initially, no biological materials can be used (proteins, cells, bioactive substances)

Lithography-based Additive Manufacturing of Calcium phoshate based implants

Debinding and sintern yields in:

1. no biological materials can be used initially (proteins, cells, bioactive substances)

2. Bioglass will transform from an amorphous to a crystalline state, will become a glass ceramic, and loose bioactivity .

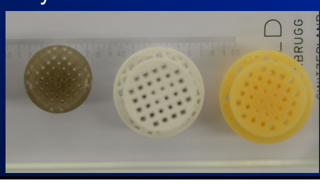

Additive Manufacturing of bone substitutes

Mechanics

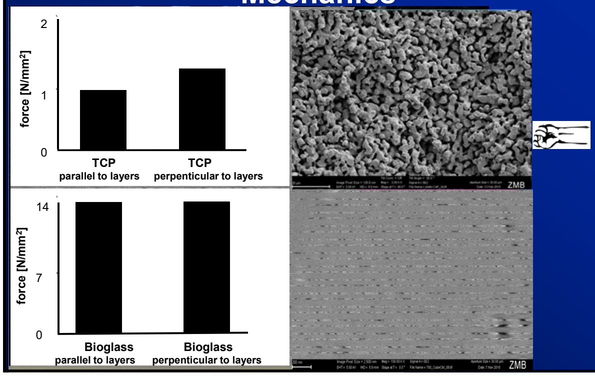

TCP 300

mechanics

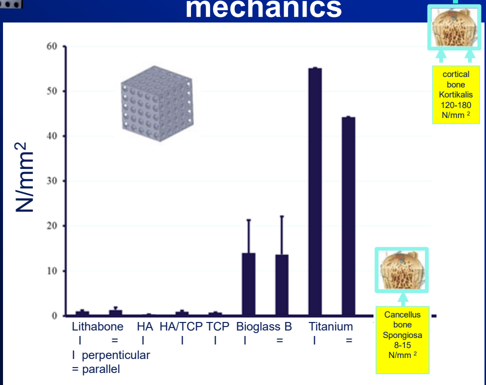

Lithography-based Additive Manufacturing of Calcium phoshate based implants

Debinding and sintering yields in:

446 T. Goto et al.: Resorption of synthetic porous HA

Table 1. Review of biodegradability of synthetic HA materials and their features

Investigator	Year	Subject	Sintering temperature	Porosity	Pore diameter (μm)	Follow-up period	Biodegradable
Winter et al.[20]	1981	Rat	900°C	1%	?	1 m–6 m	Yes
		Rat	1200°C	1%	?	1 m–6 m	Yes
		Rat	1200°C–1300°C	1%	?	1 m–6 m	No
		Rat	1200°C–1300°C	20%	?	1 m–6 m	?
		Rat	1200°C–1300°C	40%	?	1 m–6 m	?
Klein et al.[8]	1983	Rabbit	1100°C	40%	?	9 m	No
		Rabbit	1300°C	3%	?	9 m	No
Hoogendoorn et al.[5]	1984	Dog	1300°C	56%	480	≤3.5 y	No
Renooij et al.[13]	1985	Dog	1300°C	56%	180	1 y	No
van Blitterswijk et al.[18]	1985	Rat	?	26%	100	1 w–1 y	Yes
		Rat	?	<5%	3	1 w–1 y	Yes
van Blitterswijk et al.[19]	1986	Rat	?	26%	100	1 w–1 y	Yes
Kurosawa et al.[11]	1987	Human	900°C	82%	280	1 y 3 m	Yes
Kurosawa et al.[12]	1989	Dog	900°C	85%	282	2 y	Yes
		Dog	1200°C	85%	230	2 y	Yes
Uchida et al.[16]	1990	Human	1200°C	55%	?	6 m–5 y	Very slightly
Inoue et al.[6]	1993	Human	900°C	70%	90	1 y 3 m–3 y 4 m	Yes
Ukegawa et al.[17]	1995	Human	900°C	70%	90 or 200	5 y–7 y 9 m	Yes
Yoshida et al.[21]	1995	Human	900°C	70%	90 or 200	5 y–8 y 2 m	Yes
Ubayama et al.[15]	1997	Human	900°C	70%	90 or 200	6 m–8 y 5 m	Yes

HA, Hydroxyapatite: ?, not stated; m, month; y, year; w, week

Lithography-based Additive Manufacturing of Calcium phoshate based implants

Demand for debinding and sintern yields in:

1. no biological materials can be incorperated initially (proteins, cells, bioactive substances)
2. Bioglass will transform from an amorphes to a crystalline state, will become a glass ceramic, and loose bioactivity (above 500ºC.)
3. Calcium phosphates (HA) will loose their degradability, since temperatures above 900ºC will increase crystal size and favors crystal perfection.

TCP-based scaffolds

Pores and bottlenecks

de Wild, Schumacher,…. Weber FE 3D printing and additive manufacturing (2016)

Switzerland is famous for porous products

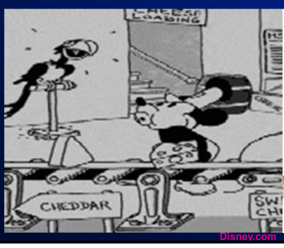

Disney.com

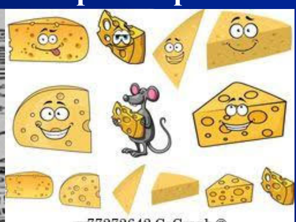

gg77272642 GoGraph ©

TCP-based scaffolds

Pores and bottlenecks

de Wild, Schumacher,…. Weber FE 3D printing and additive manufacturing (2016)

Basic design elements influence

stiffness anisotropy

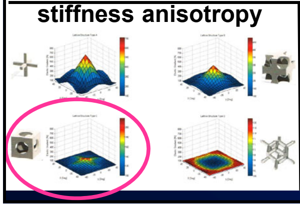

mechanics

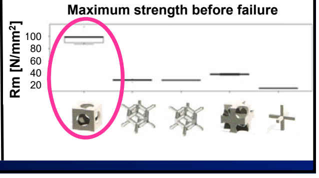

TCP-based scaffolds

Pores and bottlenecks

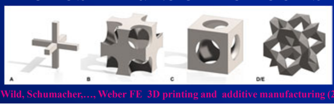

de Wild, Schumacher,…, Weber FE 3D printing and additive manufacturing (2016)

Solid works

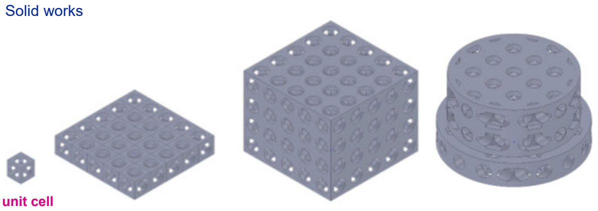

Ghayor & Weber FE Frontiers in Physiology (2018); patent pending

TCP-based scaffolds

Pores and bottlenecks

acronym	length of unit cell [mm]	pore diameter [mm]	bottleneck diameter [mm]	porosity [%]	Maximal transparency [%]
C_10_5_5	1.0	0.5	0.5	35.95	19.64
C_10_07_05	1.0	0.7	0.5	47.40	19.64
C_10_07_07	1.0	0.7	0.7	52.58	38.48
C_13_10_05	1.3	1.0	0.5	47.40	11.61
C_13_10_07	1.3	1.0	0.7	39.59	22.77
C_13_10_10	1.3	1.0	1.0	56.00	46.47
C_15_12_05	1.5	1.2	0.5	32.04	8.72
C_15_12_07	1.5	1.2	0.7	37.06	17.10
C_15_12_10	1.5	1.2	1.0	47.47	34.90
C_15_12_12	1.5	1.2	1.2	56,96	50.26
C_18_15_12	1.8	1.5	1.2	47.46	34.90
C_20_17_05	2.0	1.7	0.5	35.64	2.42
C_20_17_07	2.0	1.7	0.7	36.46	9.62
C_20_17_12	2.0	1.7	1.2	44.87	28.27
C_20_17_15	2.0	1.7	1.5	52.03	44.17

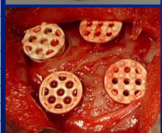

Ghayor & Weber FE Frontiers in Physiology (2018)

TCP-based scaffolds

Pores and bottlenecks

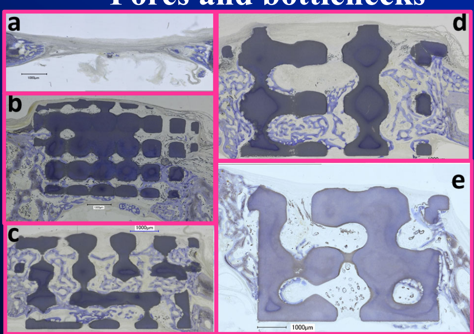

Ghayor & Weber FE Frontiers in Physiology (2018)

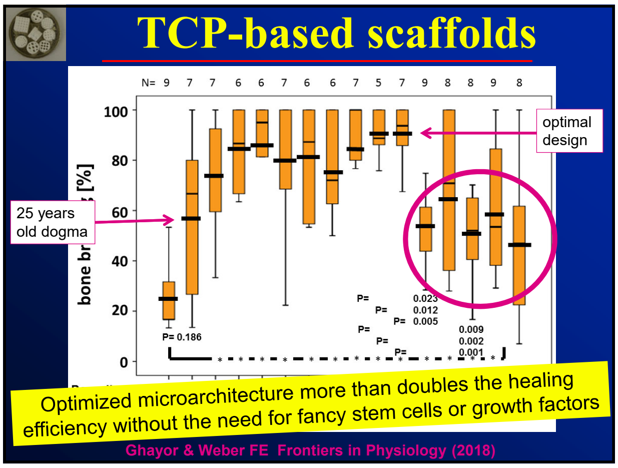
TCP-based scaffolds
N= 9 7 7 6 6 7 6 6 7 5 7 9 8 8 9 8
bone b[...] [%]
25 years old dogma
optimal design
P= 0.186
P= 0.023
P= 0.012
P= 0.005
P= 0.009
P= 0.002
P= 0.001
Optimized microarchitecture more than doubles the healing efficiency without the need for fancy stem cells or growth factors
Ghayor & Weber FE Frontiers in Physiology (2018)

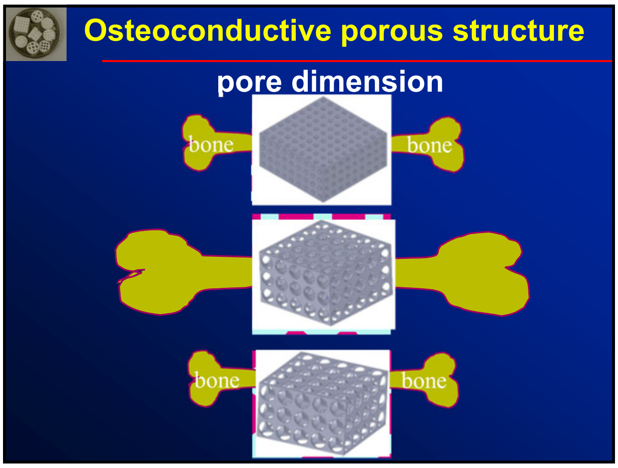
Osteoconductive porous structure
pore dimension
bone
bone
bone
bone

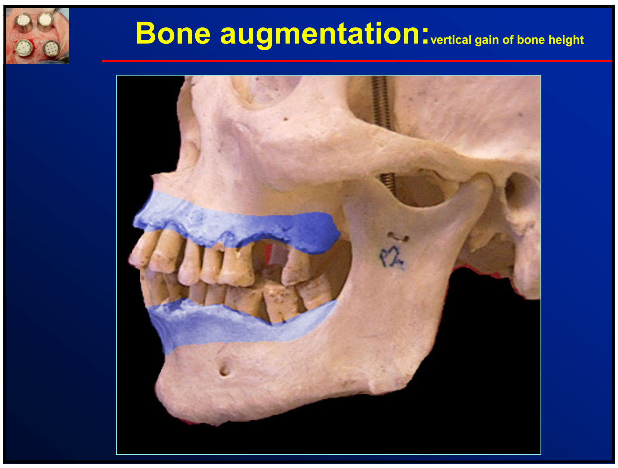
Bone augmentation: vertical gain of bone height

Bone augmentation

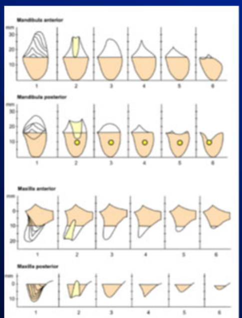

1 // Klassifikation nach Cawood und Howell [4]: 1 bezahnter Kiefer, 2 Kiefer direkt nach Extraktion, 3 abgerundeter Alveolarfortsatz, Höhe und Breite erhalten, 4 Spitzkamm, Höhe erhalten, Breite reduziert, 5 in Höhe und Breite reduzierter Alveolarfortsatz, 6 vollständig, bis unter basalen Knochen atrophierter Alveolarfortsatz

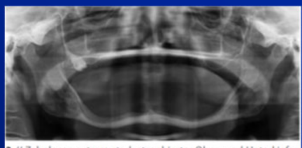
3 // Zahnloser, extrem stark atrophierter Ober- und Unterkiefer, retinierter und kariöser Zahn 18

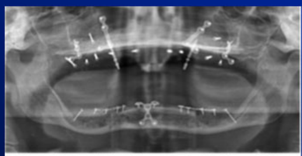
6 // Kontrollröntgenbild nach Augmentation des Ober- und Unterkiefers und der Insertion von zwei provisorischen Implantaten in Regiones 13, 23 sowie operativer Entfernung von Zahn 18

Brown & Terhyden der junge Zahnarzt 2/2018

Bone augmentation

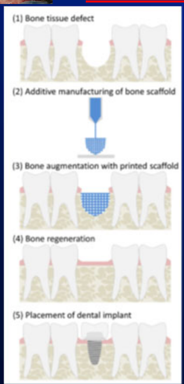

Preclinical model for bone augmentation

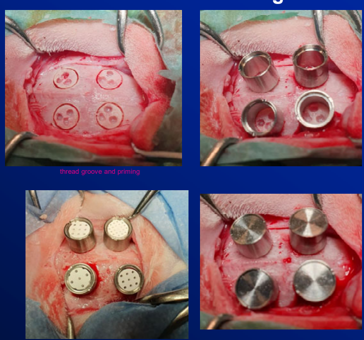

Rieder et al (2018) IJMS

Ghayor et al… Weber FE Materials&Design (2021)

Models for Osteoconduction and bone augmentation

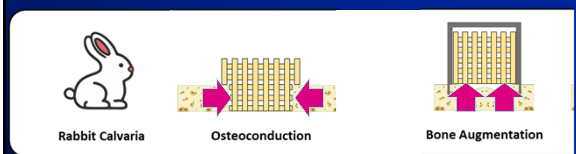

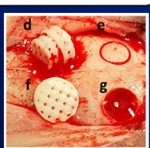

Bone augmentation

Pore design

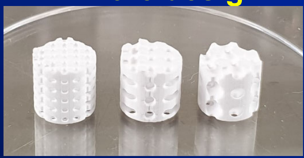

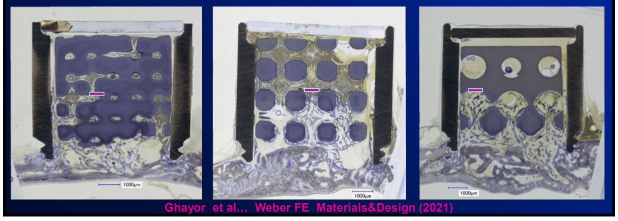

Ghayor et al… Weber FE Materials&Design (2021)

Bone augmentation

Pore design

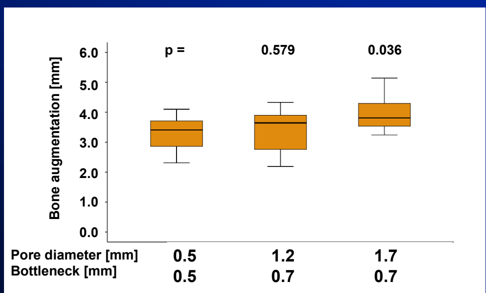

Ghayor et al… Weber FE Materials&Design (2021)

Augmentation/osteoconduction

Pore design

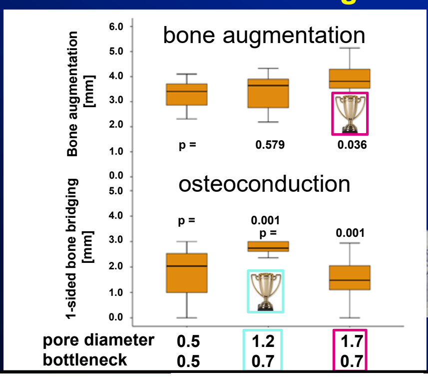

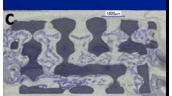

Ghayor et al…
Weber FE
Materials&Design (2021)

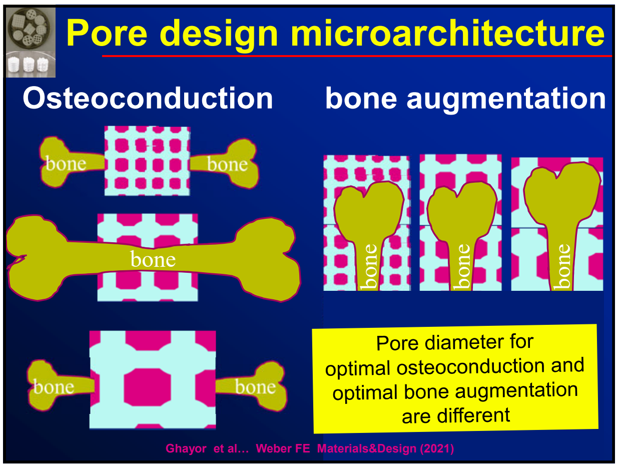
Pore design microarchitecture
Osteoconduction
bone augmentation
bone
bone
bone
bone
bone
bone
bone
bone
Pore diameter for optimal osteoconduction and optimal bone augmentation are different
Ghayor et al… Weber FE Materials&Design (2021)

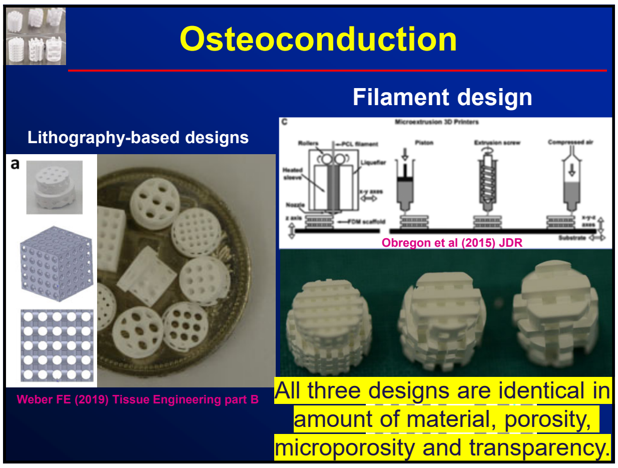
Osteoconduction
Filament design
Lithography-based designs
a
Obregon et al (2015) JDR
Weber FE (2019) Tissue Engineering part B
All three designs are identical in amount of material, porosity, microporosity and transparency.

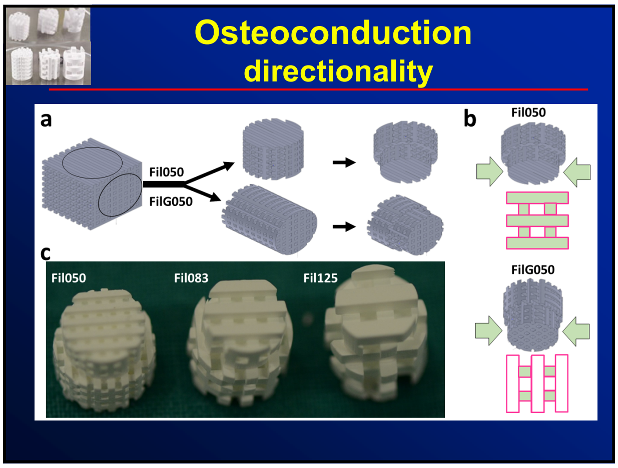
Osteoconduction
directionality
a
Fil050
FilG050
b
Fil050
FilG050
c
Fil050
Fil083
Fil125

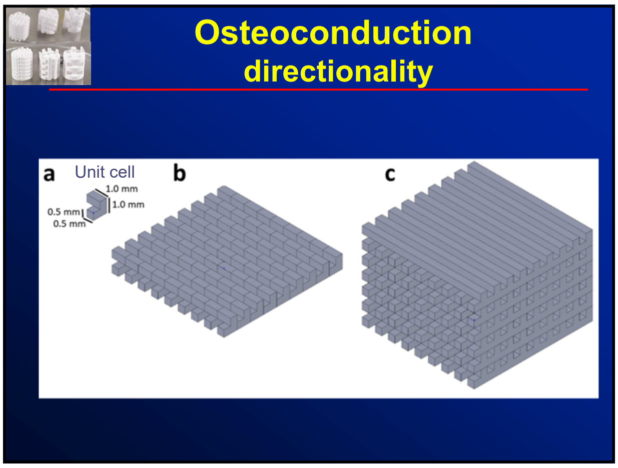
Osteoconduction
directionality
a
Unit cell
1.0 mm
1.0 mm
0.5 mm
0.5 mm
b
c

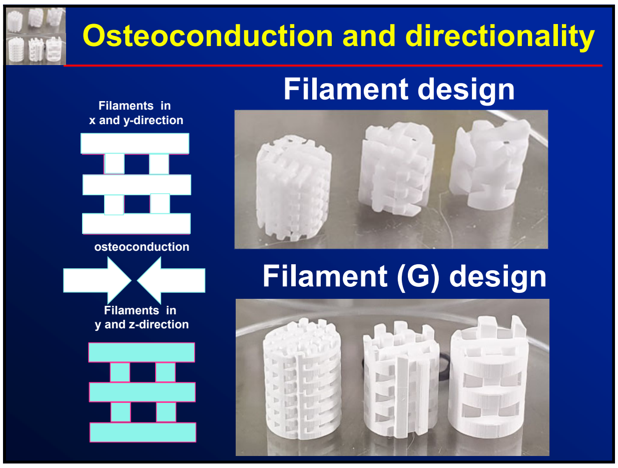
Osteoconduction and directionality
Filament design
Filaments in
x and y-direction
osteoconduction
Filaments in
y and z-direction
Filament (G) design

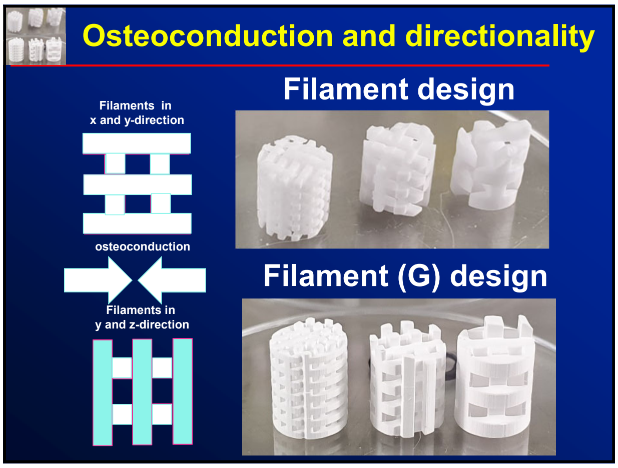
Osteoconduction and directionality
Filament design
Filaments in
x and y-direction
osteoconduction
Filaments in
y and z-direction
Filament (G) design

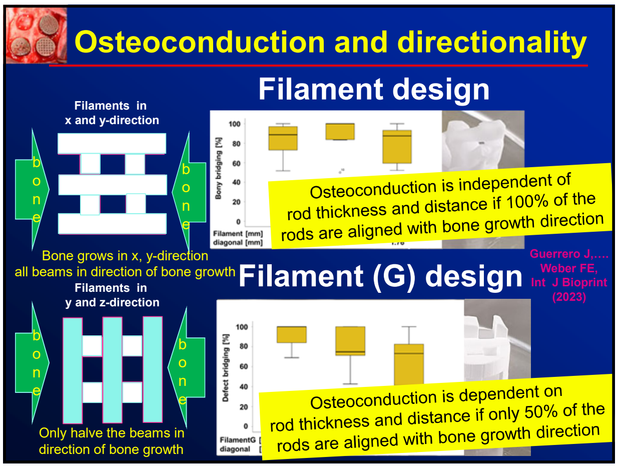
Osteoconduction and directionality
Filament design
Filaments in x and y-direction
bone
bone
Bone grows in x, y-direction
all beams in direction of bone growth
Bony bridging [%]
Osteoconduction is independent of rod thickness and distance if 100% of the rods are aligned with bone growth direction
Filament (G) design
Guerrero J,.... Weber FE, Int J Bioprint (2023)
Filaments in y and z-direction
bone
bone
Defect bridging [%]
Osteoconduction is dependent on rod thickness and distance if only 50% of the rods are aligned with bone growth direction
Only halve the beams in direction of bone growth

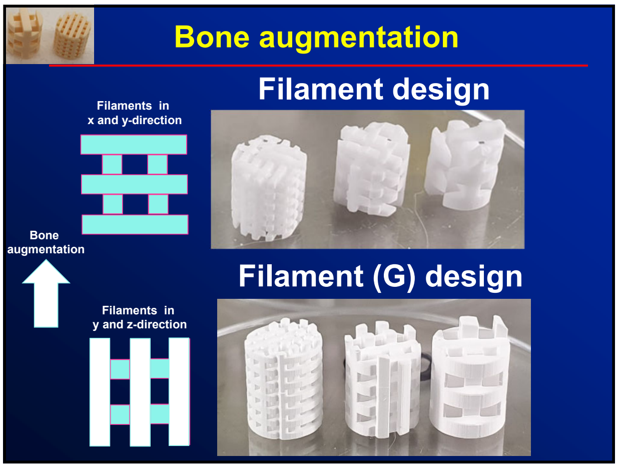
Bone augmentation
Filament design
Filaments in x and y-direction
Bone augmentation
Filament (G) design
Filaments in y and z-direction

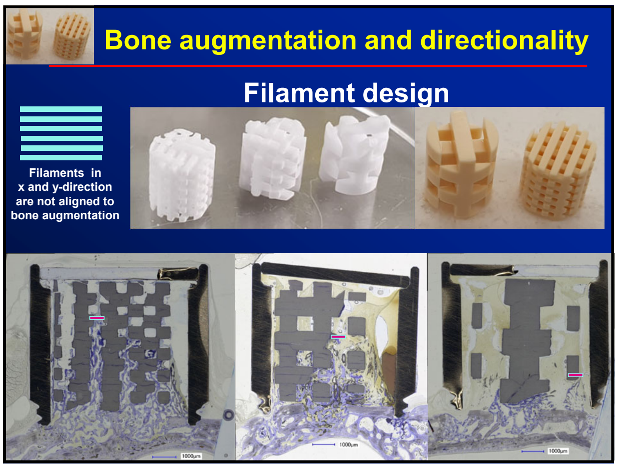
Bone augmentation and directionality
Filament design
Filaments in x and y-direction are not aligned to bone augmentation

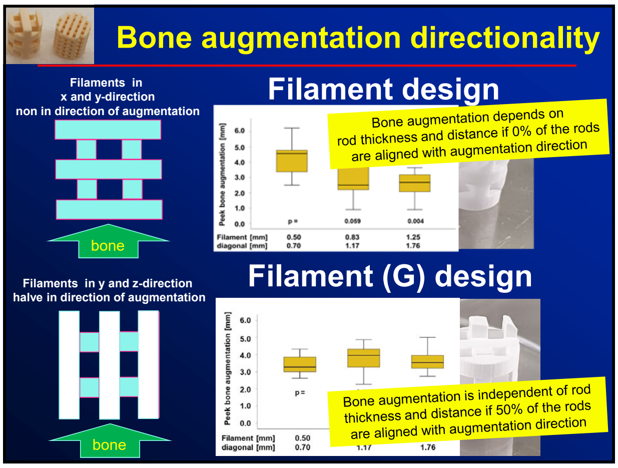
Bone augmentation directionality
Filaments in
x and y-direction
non in direction of augmentation
bone
Filament design
Bone augmentation depends on rod thickness and distance if 0% of the rods are aligned with augmentation direction
Peak bone augmentation [mm]
6.0
5.0
4.0
3.0
2.0
1.0
0.0
p =
0.059
0.004
Filament [mm]
0.50
0.83
1.25
diagonal [mm]
0.70
1.17
1.76
Filaments in y and z-direction
halve in direction of augmentation
bone
Filament (G) design
Peak bone augmentation [mm]
6.0
5.0
4.0
3.0
2.0
1.0
0.0
p =
Bone augmentation is independent of rod thickness and distance if 50% of the rods are aligned with augmentation direction
Filament [mm]
0.50
diagonal [mm]
0.70
1.17
1.76

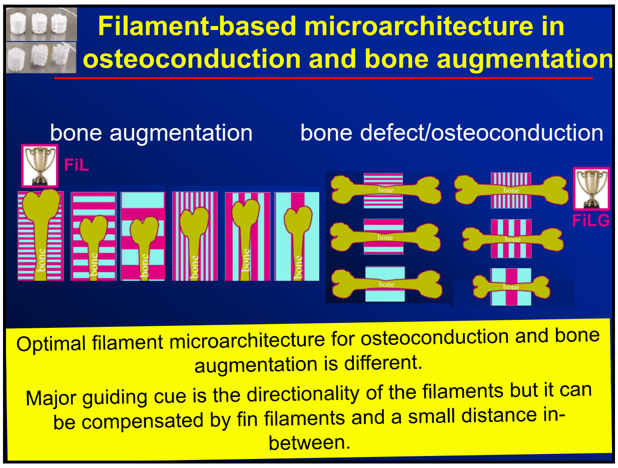
Filament-based microarchitecture in
osteoconduction and bone augmentation
bone augmentation
bone defect/osteoconduction
FiL
FiLG
Optimal filament microarchitecture for osteoconduction and bone augmentation is different.
Major guiding cue is the directionality of the filaments but it can be compensated by fin filaments and a small distance in-between.

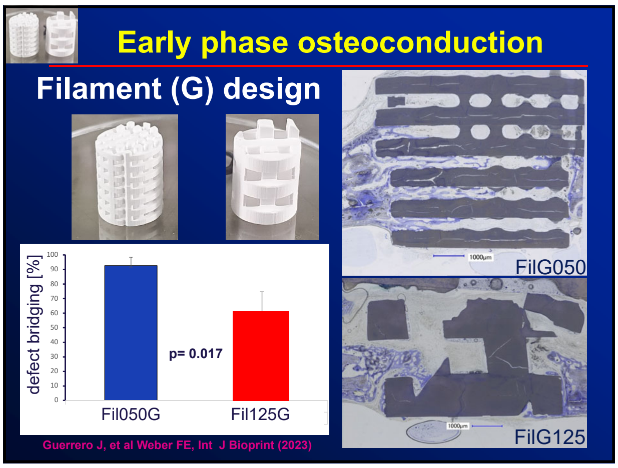
Early phase osteoconduction
Filament (G) design
defect bridging [%]
100
90
80
70
60
50
40
30
20
10
0
p= 0.017
Fil050G
Fil125G
FilG050
FilG125
Guerrero J, et al Weber FE, Int J Bioprint (2023)

Early phase osteoconduction

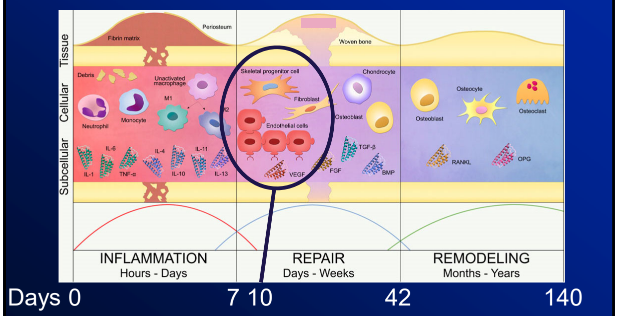

Lafuente-Gracias Front. Bioeng. Biotechnol., Volume 9 - 2021 | https://doi.org/10.3389

Microarchitecture induced early phase mesenchymal stromal cell differentiation

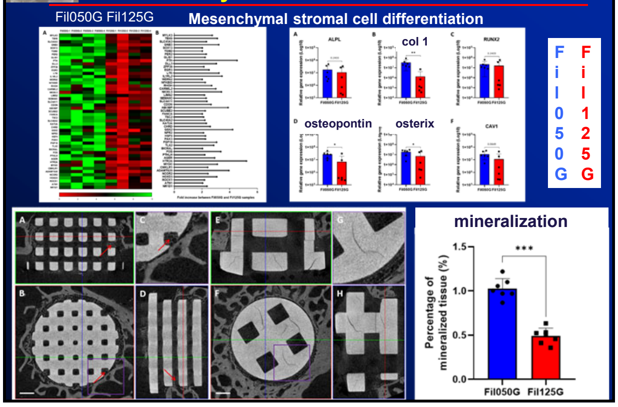

Microarchitecture induced early phase angiogenesis and vascularization

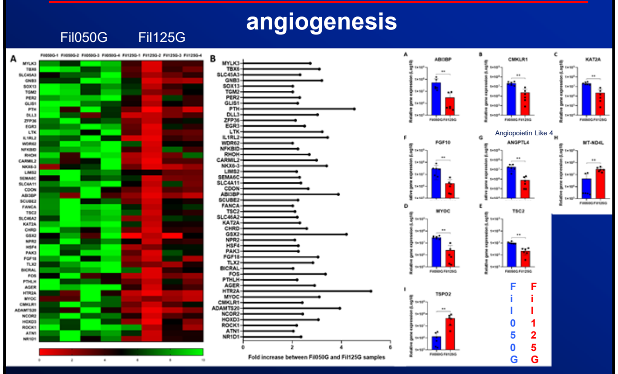

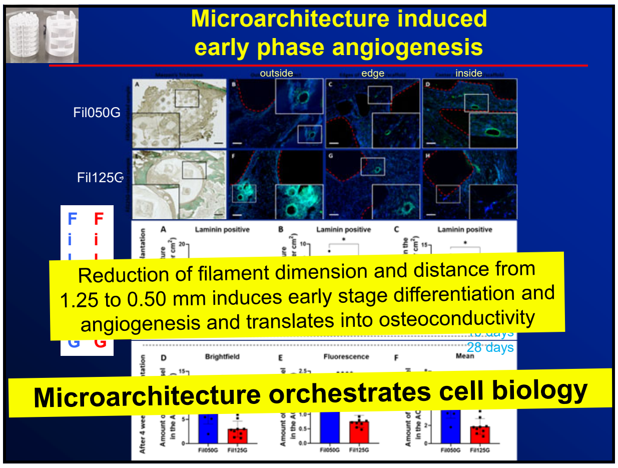
Microarchitecture induced
early phase angiogenesis
outside
edge
inside
Fil050G
Fil125G
Laminin positive
Reduction of filament dimension and distance from 1.25 to 0.50 mm induces early stage differentiation and angiogenesis and translates into osteoconductivity
28 days
Brightfield
Fluorescence
Mean
Microarchitecture orchestrates cell biology
Fil050G
Fil125G

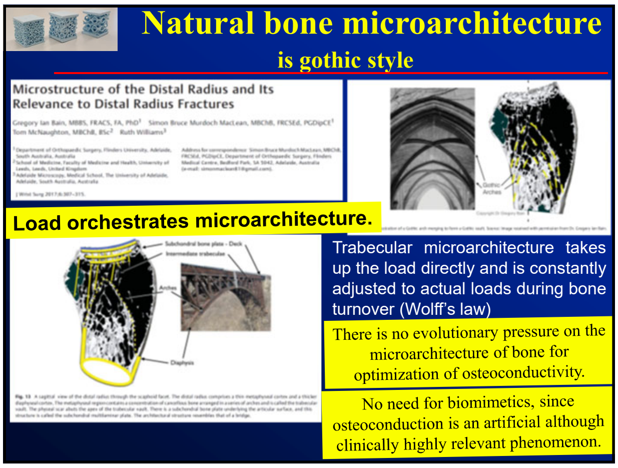
Natural bone microarchitecture
is gothic style
Microstructure of the Distal Radius and Its Relevance to Distal Radius Fractures
Load orchestrates microarchitecture.
Trabecular microarchitecture takes up the load directly and is constantly adjusted to actual loads during bone turnover (Wolff's law)
There is no evolutionary pressure on the microarchitecture of bone for optimization of osteoconductivity.
No need for biomimetics, since osteoconduction is an artificial although clinically highly relevant phenomenon.

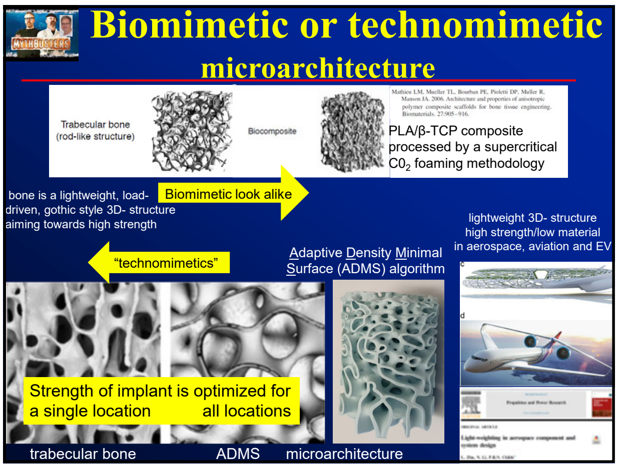
Biomimetic or technomimetic
microarchitecture
Trabecular bone
(rod-like structure)
Biocomposite
PLA/β-TCP composite processed by a supercritical C0₂ foaming methodology
bone is a lightweight, load-driven, gothic style 3D- structure aiming towards high strength
Biomimetic look alike
lightweight 3D- structure
high strength/low material
in aerospace, aviation and EV
"technomimetics"
Adaptive Density Minimal Surface (ADMS) algorithm
Strength of implant is optimized for
a single location
all locations
trabecular bone
ADMS
microarchitecture

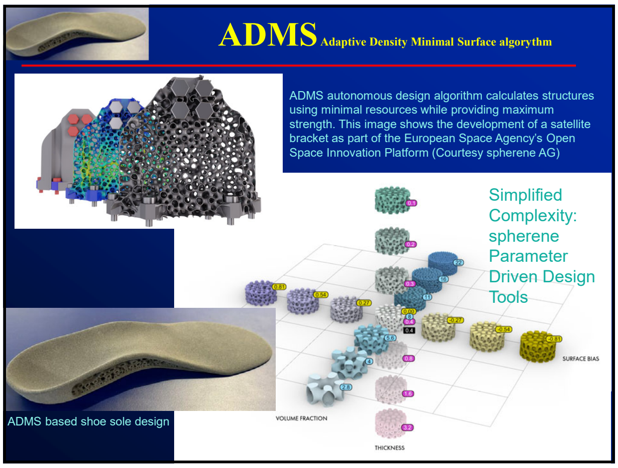
ADMS Adaptive Density Minimal Surface algorythm
ADMS autonomous design algorithm calculates structures using minimal resources while providing maximum strength. This image shows the development of a satellite bracket as part of the European Space Agency's Open Space Innovation Platform (Courtesy spherene AG)
Simplified Complexity: spherene Parameter Driven Design Tools
SURFACE BIAS
VOLUME FRACTION
THICKNESS
ADMS based shoe sole design

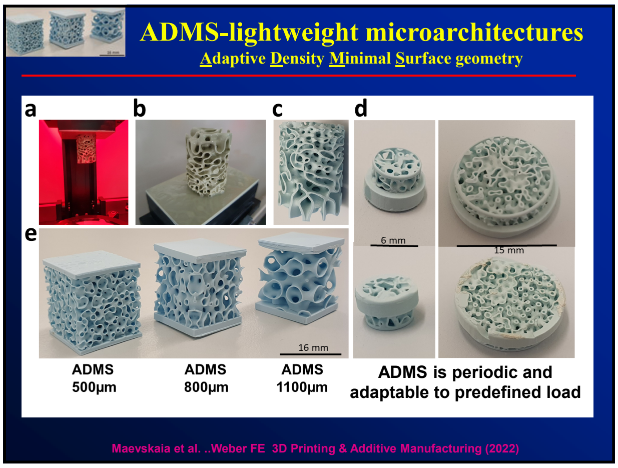
ADMS-lightweight microarchitectures
Adaptive Density Minimal Surface geometry
a
b
c
d
e
6 mm
15 mm
16 mm
ADMS 500µm
ADMS 800µm
ADMS 1100µm
ADMS is periodic and adaptable to predefined load
Maevskaia et al. ..Weber FE 3D Printing & Additive Manufacturing (2022)

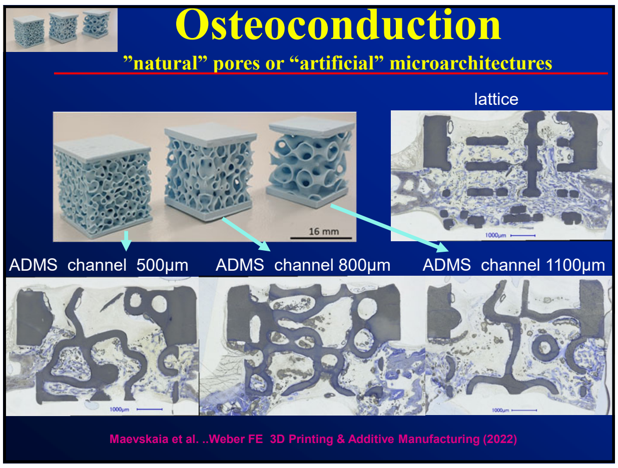
Osteoconduction
"natural" pores or "artificial" microarchitectures
lattice
16 mm
ADMS channel 500µm
ADMS channel 800µm
ADMS channel 1100µm
Maevskaia et al. ..Weber FE 3D Printing & Additive Manufacturing (2022)

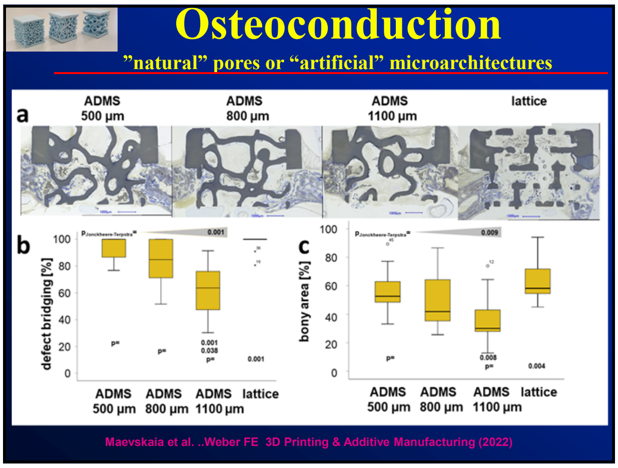
Osteoconduction
"natural" pores or "artificial" microarchitectures
a
ADMS 500 µm
ADMS 800 µm
ADMS 1100 µm
lattice
b
defect bridging [%]
100
80
60
40
20
0
0.001
0.001
0.038
0.001
ADMS 500 µm
ADMS 800 µm
ADMS 1100 µm
lattice
c
bony area [%]
100
80
60
40
20
0
0.009
0.008
0.004
ADMS 500 µm
ADMS 800 µm
ADMS 1100 µm
lattice
Maevskaia et al. ..Weber FE 3D Printing & Additive Manufacturing (2022)

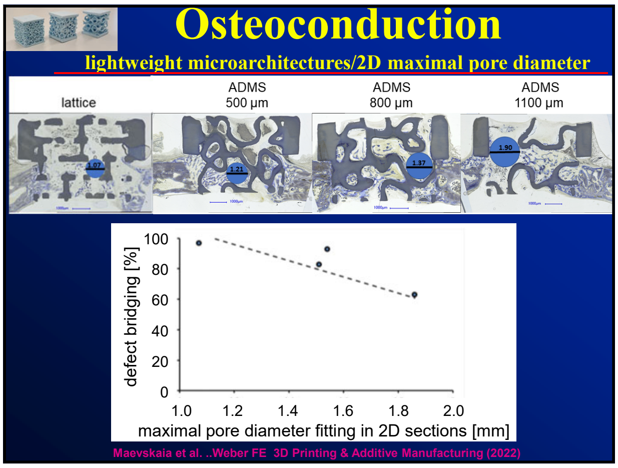
Osteoconduction
lightweight microarchitectures/2D maximal pore diameter
lattice
ADMS 500 µm
ADMS 800 µm
ADMS 1100 µm
1.90
defect bridging [%]
100
80
60
40
20
0
1.0
1.2
1.4
1.6
1.8
2.0
maximal pore diameter fitting in 2D sections [mm]
Maevskaia et al. ..Weber FE 3D Printing & Additive Manufacturing (2022)

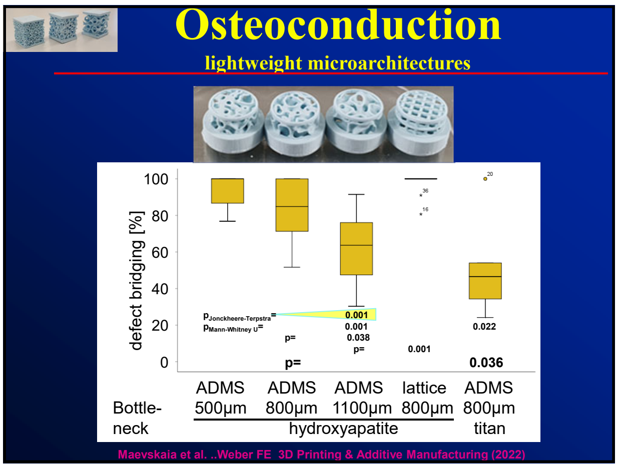
Osteoconduction
lightweight microarchitectures
defect bridging [%]
100
80
60
40
20
0
0.001
0.001
0.038
0.001
0.022
p=
p=
0.036
ADMS 500µm
ADMS 800µm
ADMS 1100µm
lattice 800µm
ADMS 800µm
Bottle-neck
hydroxyapatite
titan
Maevskaia et al. ..Weber FE 3D Printing & Additive Manufacturing (2022)

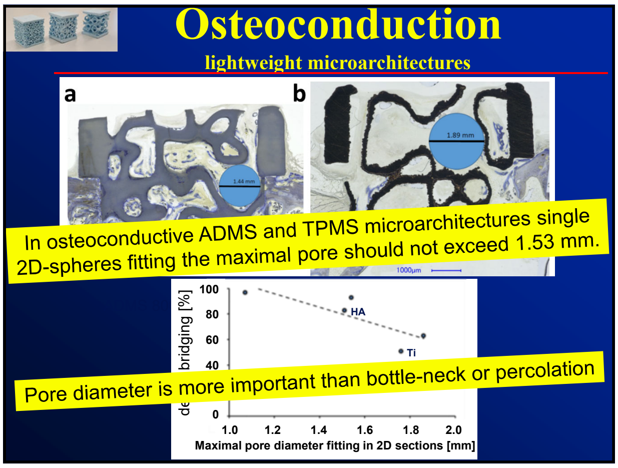
Osteoconduction
lightweight microarchitectures
a
b
In osteoconductive ADMS and TPMS microarchitectures single 2D-spheres fitting the maximal pore should not exceed 1.53 mm.
HA
Ti
Pore diameter is more important than bottle-neck or percolation
Maximal pore diameter fitting in 2D sections [mm]

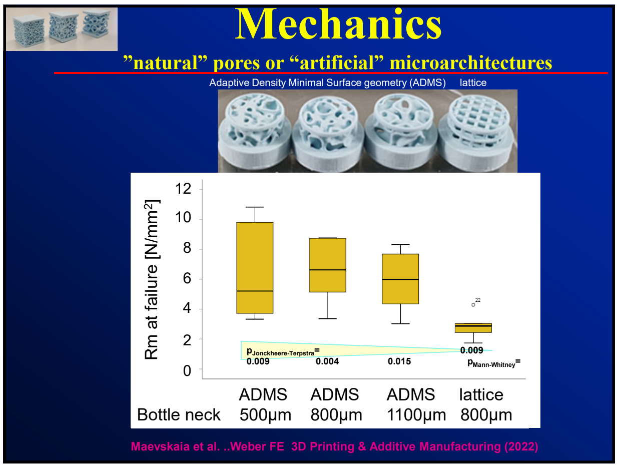
Mechanics
"natural" pores or "artificial" microarchitectures
Adaptive Density Minimal Surface geometry (ADMS)
lattice
Rm at failure [N/mm²]
Bottle neck
ADMS 500µm
ADMS 800µm
ADMS 1100µm
lattice 800µm
0.009
0.004
0.015
0.009
Maevskaia et al. ..Weber FE 3D Printing & Additive Manufacturing (2022)

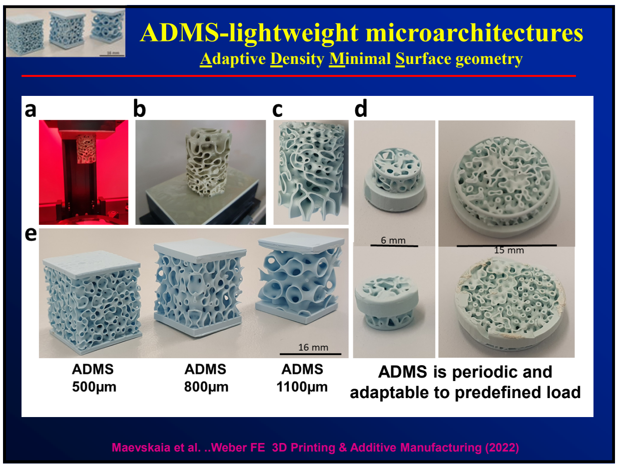
ADMS-lightweight microarchitectures
Adaptive Density Minimal Surface geometry
a
b
c
d
e
6 mm
15 mm
16 mm
ADMS 500µm
ADMS 800µm
ADMS 1100µm
ADMS is periodic and adaptable to predefined load
Maevskaia et al. ..Weber FE 3D Printing & Additive Manufacturing (2022)

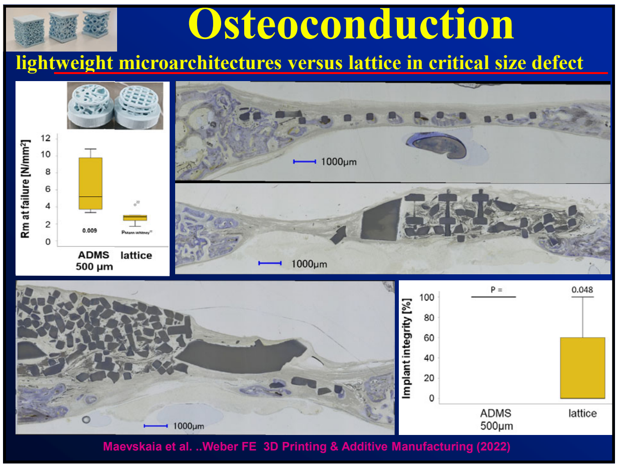
Osteoconduction
lightweight microarchitectures versus lattice in critical size defect
Rm at failure [N/mm²]
ADMS 500 µm
lattice
1000µm
1000µm
1000µm
Implant integrity [%]
0.048
ADMS 500µm
lattice
Maevskaia et al. ..Weber FE 3D Printing & Additive Manufacturing (2022)

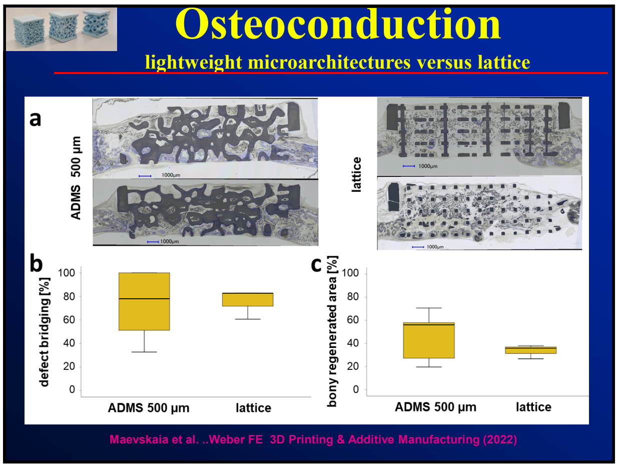
Osteoconduction
lightweight microarchitectures versus lattice
a
ADMS 500 µm
lattice
b
defect bridging [%]
ADMS 500 µm
lattice
c
bony regenerated area [%]
ADMS 500 µm
lattice
Maevskaia et al. ..Weber FE 3D Printing & Additive Manufacturing (2022)

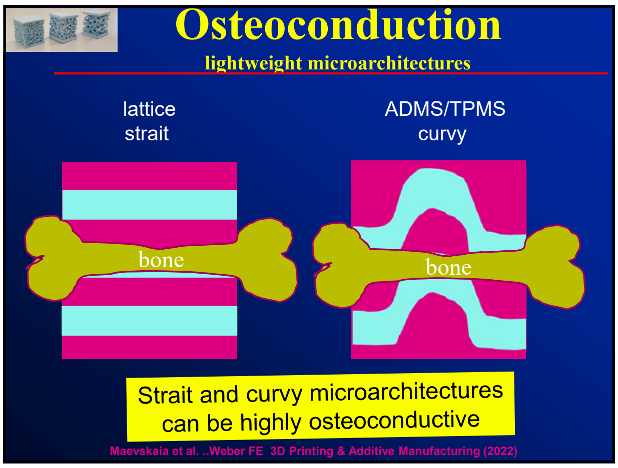
Osteoconduction
lightweight microarchitectures
lattice
strait
ADMS/TPMS
curvy
bone
bone
Strait and curvy microarchitectures can be highly osteoconductive
Maevskaia et al. ..Weber FE 3D Printing & Additive Manufacturing (2022)

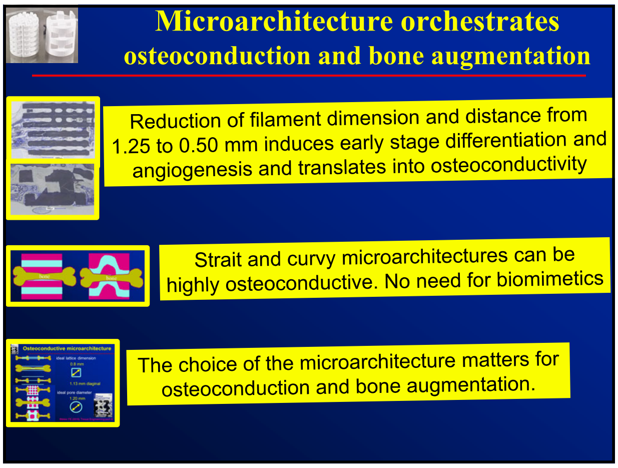
Microarchitecture orchestrates
osteoconduction and bone augmentation
Reduction of filament dimension and distance from 1.25 to 0.50 mm induces early stage differentiation and angiogenesis and translates into osteoconductivity
Strait and curvy microarchitectures can be highly osteoconductive. No need for biomimetics
The choice of the microarchitecture matters for osteoconduction and bone augmentation.


University Hospital Zurich
Center of Dental Medicine
Thank you
Center of Dental Medicine
Cranio-Maxillofacial and Oral Surgery
Oral Biotechnology & Bioengineering
Zurich, Switzerland
Chafik Ghayor
Indranil Bhattacharya
Ekaterina Maevskaia
Julien Guerrero
Ana Perez
Center of Dental Medicine
Clinic of Reconstructive Dentistry
Mutlu Ozcan
University of Applied Sciences
Northwestern Switzerland
Muttenz, Switzerland
Michael de Wild
Daniel Seiler
University Hospital
Zurich, Switzerland
BZL
Flora Nicholls
Lithoz
Vienna, Austria
Johannes Homa
Martin Schwentenwein
Spherene
Zurich, Switzerland
Christian Waldvogel
Daniel Salamon
Niklaus Arn
for your attention

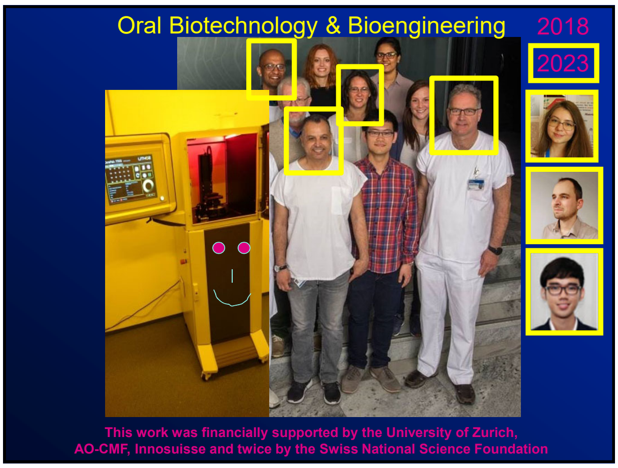
Oral Biotechnology & Bioengineering
2018
2023
This work was financially supported by the University of Zurich,
AO-CMF, Innosuisse and twice by the Swiss National Science Foundation